RESEARCH ARTICLE

WILEY

Screening and identification of biomarkers associated with the immune infiltration of intracerebral hemorrhage

Hao Guo[1,2] | Yanjun Zhang[1,3] | Zhanfei Hu[1,4] | Li Wang[1] | Hongyin Du[1] (ID)

[1]The First Central Clinical School, Tianjin Medical University, Tianjin, China

[2]Department of Anesthesiology, Shanxi provincial people's Hospital, Taiyuan, China

[3]Department of Anesthesiology, Tianjin Children's Hospital, Tianjin, China

[4]Department of Anesthesiology, Chifeng Municipal Hospital, Chifeng, China

Correspondence
Hongyin Du, The First Central Clinical School, Tianjin Medical University, No.24 Fukang Road, Nankai District, Tianjin 300192, China.
Email: duhongyin999@sina.com

Abstract

Background: Recent studies showed that inflammation and immunity might play essential roles in the progression of intracerebral hemorrhage (ICH). However, the underlying mechanisms for changes at the cellular and molecular levels after ICH remain unclear.

Methods: We downloaded the microarray dataset of ICH from the Gene Expression Omnibus (GEO) database. The differential expression gene analysis was obtained by weighted gene co-expression network analysis (WGCNA). We got the hub genes and performed the biological functions and signaling pathways of these genes by Metascape. GSVA algorithm was used to evaluate the potential physical function of time-varying ICH samples. We used single-sample gene set enrichment analysis (ssGSEA) to assess the immune signatures infiltration and analyzed the correlation between hub genes and immune signatures.

Results: The data sets of all 22 ICH samples in GSE125512 were examined by the WGCNA R package. We finally screened five hub genes (GAPDH, PF4, SELP, APP, and PPBP) in the royal blue module. Metascape analysis displayed the biological processes related to inflammation and immunology. Cell adhesion molecule binding, myeloid leukocyte activation, CXCR chemokine receptor binding, and regulation of cytokine production were the most enriched pathophysiological process. The immune signatures infiltration analyses showed that ICH patients' early and late samples had different activity and abundance of immune-related cells and types.

Conclusions: GAPDH, PF4, SELP, APP, and PPBP are identified as potential biomarkers for predicting the progression of ICH. This study may help us better understand the immunologic mechanism and shed new light on the promising approaches of immunotherapy for ICH patients.

KEYWORDS
bioinformatics analysis, gene expression omnibus, immune infiltration, intracerebral hemorrhage, weighted gene co-expression network analysis

1 | INTRODUCTION

Intracerebral hemorrhage (ICH) remains the most devastating form of stroke.[1] Although ICH accounts for 10%–15% of all stokes, it is reported that the fatality rate of ICH at 30 days is approximately 40%, and a 1-year survival rate of only 30%.[2,3] It has caused a severe concern for public health, and patients who are suffering from ICH will have severe neurological deficits, causing a substantial burden on both parents and families.

Intracerebral hemorrhage is defined as the nontraumatic hemorrhage of the primary brain parenchyma. ICH is caused by the spontaneous infiltration of blood into the brain parenchyma.[4] Previous preclinical and a few clinical studies implicate that secondary brain injury might accelerate the progression of ICH.[5,6] Secondary damage following ICH is triggered by the hematoma, which involves various complex pathological processes, such as brain edema, blood-brain barrier destruction, inflammation, and neuronal death.[7] However, the underlying mechanisms of secondary brain injury after ICH remain unclear. In recent years, growing evidence has shown that immune cell infiltration plays a vital role in the occurrence and development of ICH, especially for secondary injury and the formation of perihematomal edema. Immunomodulators have been proved to delay the progression of PHE, reduce the level of matrix metalloproteinase 9 (MMP-9) in plasma and improve the clinical outcome of ICH patients.[8,9] Treg cells (Regulatory T cells), as a negative regulatory subset of cells that can inhibit the function of other immune cells, induce the protective M2 type transformation of microglia after ICH, and inhibit the upregulation of pro-inflammatory cytokines, such as TNF-α, IL-β and MMP-2.[10]

In this study, we hypothesized that several genes could up- or downregulate in the evolving brain injury, indicating what pathophysiological mechanisms were occurring and how ICH would induce inflammatory and immunologic changes. Using bioinformatics technology, we first downloaded the microarray dataset of ICH from the Gene Expression Omnibus (GEO) database. We performed differential expression gene analysis by weighted gene co-expression network analysis (WGCNA). Subsequently, we identified the key genes and used single-sample gene set enrichment analysis (ssGSEA) to analyze the difference in immune infiltration for the first time. In addition, we analyzed the correlation between immune signatures and the expression of genes. These findings may help us better understand the pathophysiological mechanisms of brain injury by exploring the dynamic changes of core genes. Besides, from the immune system's perspective, evaluating the infiltration of immune cells and determining the differences in the composition of infiltrating immune cells are of great value for elucidating the specific molecular mechanism of ICH and developing new immunotherapeutic targets.

2 | MATERIALS AND METHODS

2.1 | Gene expression microarray data

We acquired the microarray expression profiles of intracerebral hemorrhage patients from Gene Expression Omnibus (GEO) database (http://www.ncbi.nlm.nih. gov/geo/) that contains high-throughput gene expression data, under the accession number GSE125512. Dataset GSE125512, performed on the platform of GPL15433 includes 11 patients and 22 samples. The first peripheral blood sample was obtained from each patient within 24 h of ICH symptom onset, and the second peripheral blood sample was collected from the same patient 72 h (+/− 6 h) following the first. The aligned reads were quantified and converted to relative gene expression levels represented by FPKM for the subsequent network construction.

2.2 | WGCNA and identification of clinically significant modules

Weighted gene co-expression network analysis, a systematic biology method to find the modules of highly correlated genes with clinical phenotypes.[11,12] In our study, we followed the standard process of WGCNA and applied the "WGCNA" package in R (http://www.r-project.org/) for data processing. We removed genes with zero-variance between groups and screened the top 5,000 genes invariance for further analysis. The purpose of soft threshold setting was to make the network more in line with the characteristics of the scale-free network. Then, we performed a topological overlap matrix (TOM) to estimate its connectivity and carried out hierarchical clustering analysis for dynamic tree cut. We used different colors to distinguish the modules.

Two indicators were adopted to identify modules related to clinical phenotypes. Module eigengenes (MEs) summarized all genes with similar expression patterns into a single characteristic expression profile module. Gene significance (GS) was calculated by the correlation between MEs and clinical characteristics, equal to the log10 conversion of the p-value in the linear regression between gene expression and clinical information (GS = LgP).[13] The purpose of GS was to identify the clinically relevant modules and the ME of the module was considered the one related to the clinical feature.

2.3 | Functional enrichment analysis of hub modules

Metascape (www.metascape.org)is a web-based portal that provides a comprehensive gene list annotation and analysis resource for experimental biologists.[14] Our study used the tool to perform the biological functions and signaling pathways of genes involved in hub modules. Pathway with Min Overlap ≥ 3 and $p ≤ 0.01$ was considered statistically significant. Besides, terms with similarities >0.3 were connected by edges and presented as a network graph to further explore the relationship between terms.

2.4 | Hub genes identification and efficacy verification

Hub genes are highly interconnected with nodes in the module and have been considered potential biological targets for clinical

traits corresponding to the module. Our research used the modular connectivity and clinical traits relationship to select candidate hub genes for the hub module. Here, module connectivity referred to the absolute value of the Pearson's Correlation between genes (Module Membership). The clinical trait relationship referred to the absolute value of the Pearson's Correlation between each gene and the trait (Gene Significance). We set the screening criteria (gene significance for group >0.5, module membership >0.8, and weighted Correlation <0.01) for the feature module. Moreover, we uploaded all genes in the hub module to the Search Tool for the Retrieval of Interacting Genes (STRING) database (https://string-db.org/) to construct protein–protein interaction (PPI) and obtain hub genes. We defined genes with node connectivity ≥15 as the central nodes. Cytoscape was conducted to present the network (https://cytoscape.org/).

These hub genes were verified by exploring the dynamic changes with the progression of ICH and selected for receiver operating characteristic (ROC) analysis. The area under the curve (AUC) was applied to assess each gene's performance to predict the progression of ICH.

2.5 | Gene set variation analysis (GSVA)

Gene set variation analysis is a nonparametric and unsupervised method for evaluating the enrichment of transcriptome genomes. By comprehensively scoring the gene sets of interest, it converts the gene-level changes into path-level changes and evaluates the biological function of the samples.[15] In this study, we used the GSVA algorithm to evaluate the potential biological function of time-varying ICH samples.

2.6 | Evaluation of immune signatures infiltration

We used single-sample gene set enrichment analysis (ssGSEA)[16] to obtain the chip data of patients with different subgroups of ICH. Herein, 29 immune signatures were first quantified for their enrichment degrees within respective ICH samples. We used the ssGSEA method to deduce the infiltration level of different immune cells and the activity of immune-related functions in ICH expression profile data. The samples were screened with a p-value < 0.05. Utilizing the "Corrplot" package to display a correlation heatmap to visualize the Correlation of 29 types of infiltrating immune signatures; the "ggplot2" package was used to analyze the differences in immune signatures infiltration between the two groups.

2.7 | The Correlation between hub genes and immune signatures

Spearman correlation analysis was used to perform the relationship between hub genes and infiltrating immune cells. The "ggplot2"

package was employed to exhibit the results. p-value < 0.05 was confirmed to be statistically different.

3 | RESULTS

3.1 | WGCNA and clinically significant modules identification

The data sets of all 22 ICH samples in training set GSE125512 were preprocessed to construct the co-expression module by the WGCNA R package. We obtained the gene sets for subsequent analysis by removing genes with zero-variance. The hclust function was used and the clustering dendrograms with samples were correctly sorted in random order. The result was shown in (Figure 1A). Then, we set the soft threshold (power) as 9 to make the value of scale independence exceed 0.8 and the average connectivity degree is higher (Figure 1B). Next, we used the power value to construct co-expression modules and finally identify 10 distinct gene co-expression modules in ICH (Figure 1C). These co-expression modules were shown in different colors.

According to the Correlation between traits and module feature vector genes and p-value, the ME of the royal blue module showed a higher correlation with progress than other modules (Figure 1D). Thus, we identified the royal blue module as the most relevant module to the disease progression of ICH.

3.2 | Functional enrichment analysis

Metascape analysis displayed the first 20 enriched terms as a bar graph for the biological functions and signaling pathways. The results revealed that the hub genes in the royal blue module were mainly involved in platelet alpha granule, response to wounding, anchoring junction, platelet alpha granule membrane, and so on (Figure 2A). The network diagram was constructed with each enrichment term as a node and the similarity of the node as the edge (Figure 2B). Among them, the biological processes related to inflammation and immunology were mainly enriched in cell adhesion molecule binding, myeloid leukocyte activation, CXCR chemokine receptor binding, and regulation of cytokine production. Thus, we inferred that the immune response might play an important role in ICH.

3.3 | Identification and verification of hub genes in the royal blue module

A total of five genes with the cut-off standard were identified as candidate hub genes: GAPDH, PF4, SELP, APP, and PPBP (Figure 3A). The results were consistent with the central node screened out by the PPI network we constructed (Figure 3B). With the dynamic change of the ICH process, we analyzed the differential expression of these five hub genes. These genes increased significantly with the progression of ICH, and the difference was

(A)

(B)

(C)

(D)
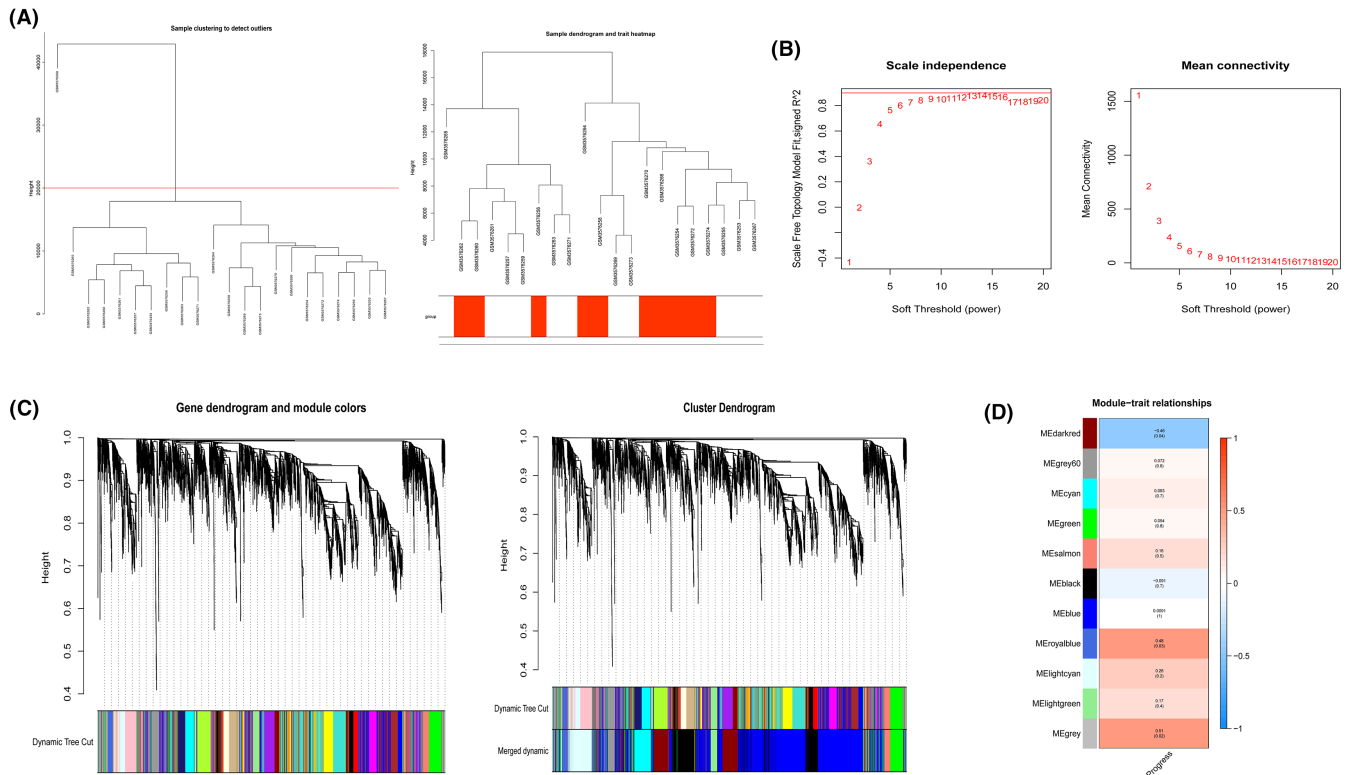
FIGURE 1 Weighted gene co-expression network analysis (WGCNA). (A) Clustering dendrogram of 22 samples. We performed sample clustering to detect outliers and confirm the removal of the batch effect from data sets. (B) The optimal soft threshold power of the WGCNA was screened by calculating the scale-free topological fit index and the average connectivity. (C) Dendrogram of all differentially expressed genes clustered according to a dissimilarity measure (1- TOM). Different colors represented the divided modules. (D) The heatmap of correlation between ME and the progress of ICH modules

statistically significant (Figure 3C–G). As an example, by comparing the drawn boxplot in the early stage (ICH within 24 h), the gene expression of GAPDH was significantly increased in the late phase (ICH at 72 h following the first time) (Figure 3C). Moreover, the AUC value of these genes was all >0.75 (Figure 3H–L) by ROC analysis, which verified that they had an excellent predictive effect on ICH progression.

3.4 | GSVA

We used the GSVA algorithm to obtain the main regulated pathways of the differences in the expression levels of hub genes with the progression of ICH. Among the abundant results in the five genes, we found several overlapping pathways related to immune and inflammation response pathways, such as TNFα signaling via NF-kappa B pathway, IL6-JAK-STAT3 signaling pathway, and IL2-STAT5- signaling pathway (Figure 4A–E).
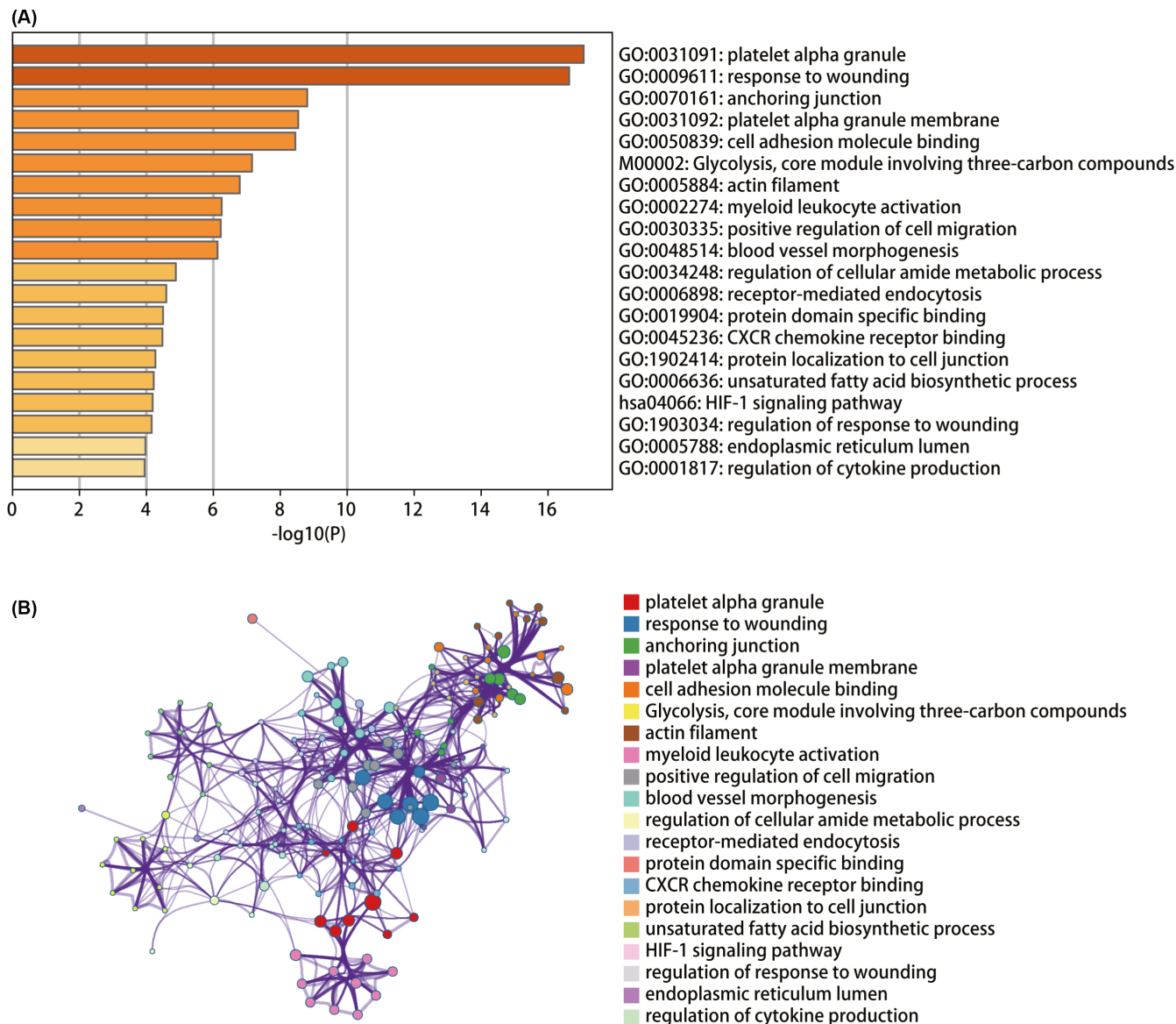
3.5 | Immune signatures infiltration analyses

Using the ssGSEA method, we first mapped the infiltration levels of 29 immune-related cells and types in all patients with ICH. The abscissa in the figure represented the number of each patient. The

vertical axis represented the value of the quantified immune signatures infiltration (Figure 5A). Similarly, the activity or abundance of immune signatures in early and late samples from patients with ICH were quantified according to the ssGSEA score, respectively. These two groups showed different activity and abundance of immune-related cells and types (Figure 5B). Correlation heatmap of the 29 types of immune signatures revealed that aDCs, APC co-inhibition, and Tregs had a significant positive correlation. ADCs and APC co-inhibition had a negative correlation with NK cells (Figure 5C). The violin plot of the immune signatures infiltration showed the difference between the two stages of ICH. Compared with the early stage of ICH, the late stage of ICH generally contained a higher proportion of aDCs and APC co-inhibition (Figure 5D, $p < 0.05$).

3.6 | Correlation analysis between hub genes and immune signatures

Correlation analysis showed that GAPDH was positively correlated with aDCs, Type-II IFN response and APC co-inhibition ($r > 0.4$, $p < 0.05$) and negatively correlated with NK cells, Cytolytic activity and Th2 cells ($r < -0.4$, $p < 0.05$) (Figure 6A). PF4 was positively correlated with Type-II IFN response and APC co-inhibition ($r > 0.4$, $p < 0.05$) (Figure 6B). Similarly, SELP was positively correlated with Type-II IFN response and APC co-inhibition ($r > 0.5$, $p < 0.05$) and

(A)

GO:0031091: platelet alpha granule
GO:0009611: response to wounding
GO:0070161: anchoring junction
GO:0031092: platelet alpha granule membrane
GO:0050839: cell adhesion molecule binding
M00002: Glycolysis, core module involving three-carbon compounds
GO:0005884: actin filament
GO:0002274: myeloid leukocyte activation
GO:0030335: positive regulation of cell migration
GO:0048514: blood vessel morphogenesis
GO:0034248: regulation of cellular amide metabolic process
GO:0006898: receptor-mediated endocytosis
GO:0019904: protein domain specific binding
GO:0045236: CXCR chemokine receptor binding
GO:1902414: protein localization to cell junction
GO:0006636: unsaturated fatty acid biosynthetic process
hsa04066: HIF-1 signaling pathway
GO:1903034: regulation of response to wounding
GO:0005788: endoplasmic reticulum lumen
GO:0001817: regulation of cytokine production

(B)

- platelet alpha granule
- response to wounding
- anchoring junction
- platelet alpha granule membrane
- cell adhesion molecule binding
- Glycolysis, core module involving three-carbon compounds
- actin filament
- myeloid leukocyte activation
- positive regulation of cell migration
- blood vessel morphogenesis
- regulation of cellular amide metabolic process
- receptor-mediated endocytosis
- protein domain specific binding
- CXCR chemokine receptor binding
- protein localization to cell junction
- unsaturated fatty acid biosynthetic process
- HIF-1 signaling pathway
- regulation of response to wounding
- endoplasmic reticulum lumen
- regulation of cytokine production

FIGURE 2 Functional enrichment analysis for the hub genes in the royal blue module. (A) The bar graph displayed the first 20 enriched terms for the biological functions and signaling pathways by Metascape analysis. (B) The network diagram was constructed with each enrichment term as a node and the similarity of the node as the edge

negatively correlated with NK cells and Th2 cells ($r < -0.4$, $p < 0.05$) (Figure 6C). APP was positively correlated with Type-II IFN response, T helper cells, APC co-inhibition, aDCs and Mast cells ($r > 0.4$, $p < 0.05$) and negatively correlated with NK cells ($r < -0.5$, $p < 0.05$) (Figure 6D). PPBP was positively correlated with Type-II IFN response and Mast cells ($r > 0.5$, $p < 0.05$) and negatively correlated with cytolytic activity and Th1 cells ($r < -0.4$, $p < 0.05$) (Figure 6E).

4 | DISCUSSION

Intracerebral hemorrhage, which accounts for 10%–15% of all stroke subtypes, is the most common type of hemorrhagic stroke. Until now, there is still no effective treatment for this devastating disorder. Patients with ICH often experience poor outcomes due to the

lack of efficient therapies. Comprehensive analysis of past studies suggests that immune responses serve a vital role in the progress of ICH.[17] Hence, identifying the immune cell infiltration characteristics has more excellent prognostics value in ICH. With the rapid development of technology, bioinformatics provides a powerful strategy for molecular marker screening. Among them, WGCNA shows unique advantages to identify modules and core genes associated with disease phenotypes. Our study deeply mined the GEO database to obtain gene expression profiles from patients with ICH and screened for hub genes. At first, we performed WGCNA to identify the critical module in the progression of ICH.

Meanwhile, we reported meaningful enrichment and pathways by metascape analysis, which triggered the regulatory ways linked to secondary cerebral injury induced by ICH. Next, we identified the five hub genes, which were involved in the pathophysiology of ICH.
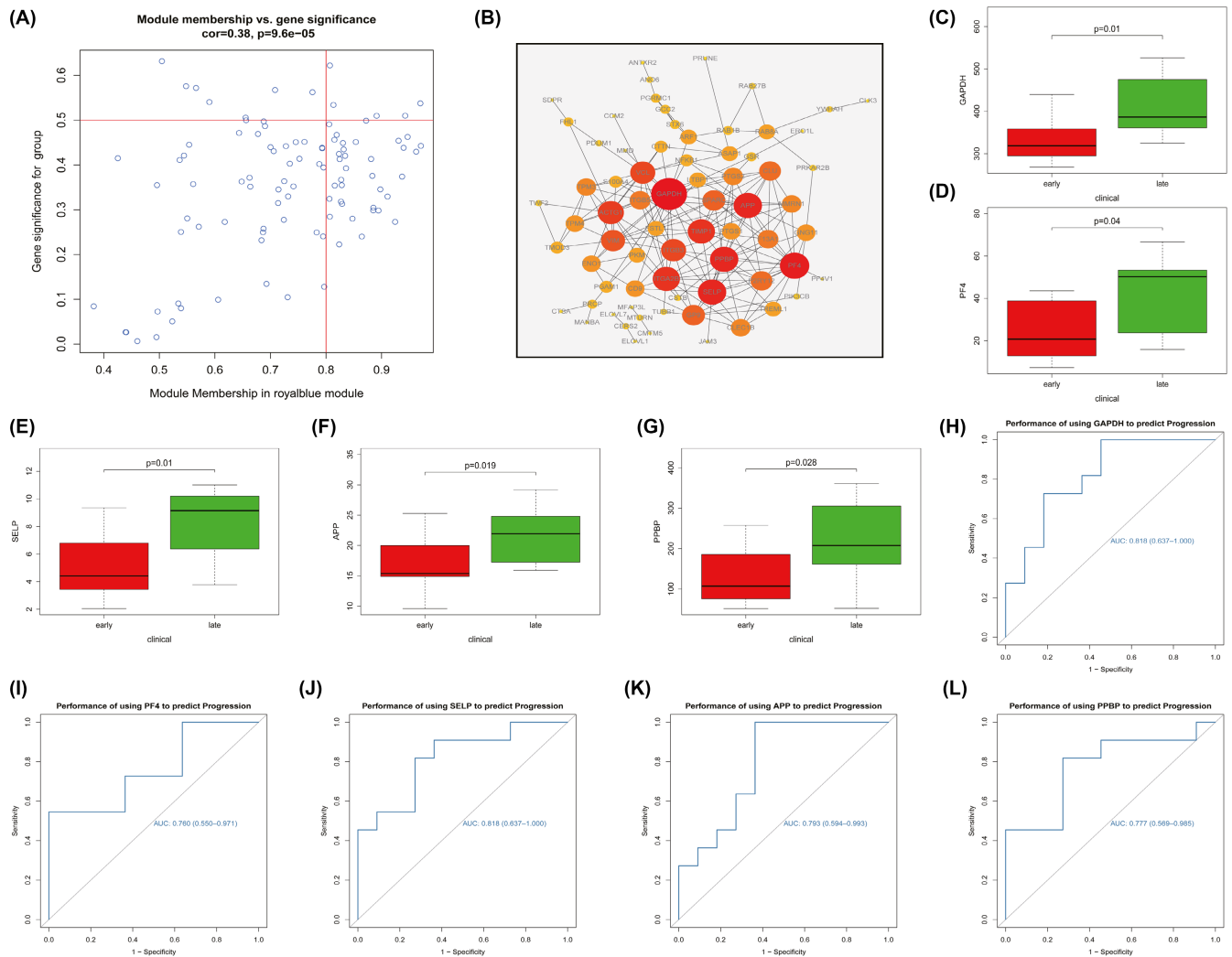
FIGURE 3 Hub genes detection and validation in the royal blue module. (A) The scatterplot of Gene Significance (GS) for a group versus Module Membership (MM) in the royal blue module. Five hub genes were selected in the royal blue module. (B) The PPI network displayed the results of the central node related to the progress of ICH. Color represented connectivity. The darker the color, the higher the connectivity (C–G). The differential expression of these five hub genes with the dynamic change of the ICH process. These genes all increased significantly in the late stage than in the early stage of ICH ($p < 0.05$). (H–L) The ROC curve showed the performance of using these five hub genes to predict progression. The AUC value of these genes was all >0.75, which verified that they had a good predictive effect on ICH progression

Then, the GSVA algorithm was applied to obtain the main regulated pathways of these five genes. Finally, we mapped the infiltration levels of immune-related cells and types in all patients using the ICH-based ssGSEA method. The above evidence provided new research ideas for clarifying the diagnostic markers of cerebral hemorrhage changes and further exploring the role of immune cell infiltration in the dynamic changes of a cerebral hemorrhage.

Intracerebral hemorrhage would induce focal inflammation in the injured cerebrum region. Such localized brain inflammation provoked secondary brain injury by magnifying blood-brain barrier (BBB) damage, cerebrum edema, oxidative stress, and directly leading to neuronal cell death. In addition to inflammation localized in the injured brain region, numerous evidences demonstrated that inflammatory responses after ICH could occur and persist throughout the entire brain. Whole brain inflammation might continuously

frame the evolving pathology following ICH and affect patients' long-term neurological outcomes.[18] In our research, five hub genes (GAPDH, PF4, SELP, APP, and PPBP) with the cut-off standard (gene significance for group >0.5, module membership >0.8, and weighted Correlation <0.01) were identified and screened out by the PPI network. GAPDH (glyceraldehyde-3-phosphate dehydrogenase) was considered a classical glycolytic protein of little interest. As a "housekeeping" protein, it has been frequently used to normalize PCR, western or northern blots for a long time. However, in recent years, the view has changed since GAPDH is now known to contribute to a number of diverse cellular functions, such as DNA replication and repair, apoptosis, neurodegenerative disease, and viral pathogenesis unrelated to glycolysis.[19] The GAPDH expressions were also differentially regulated in a variety of types of cells. The recent studies notified that GAPDH was differentially expressed in multiple tumor
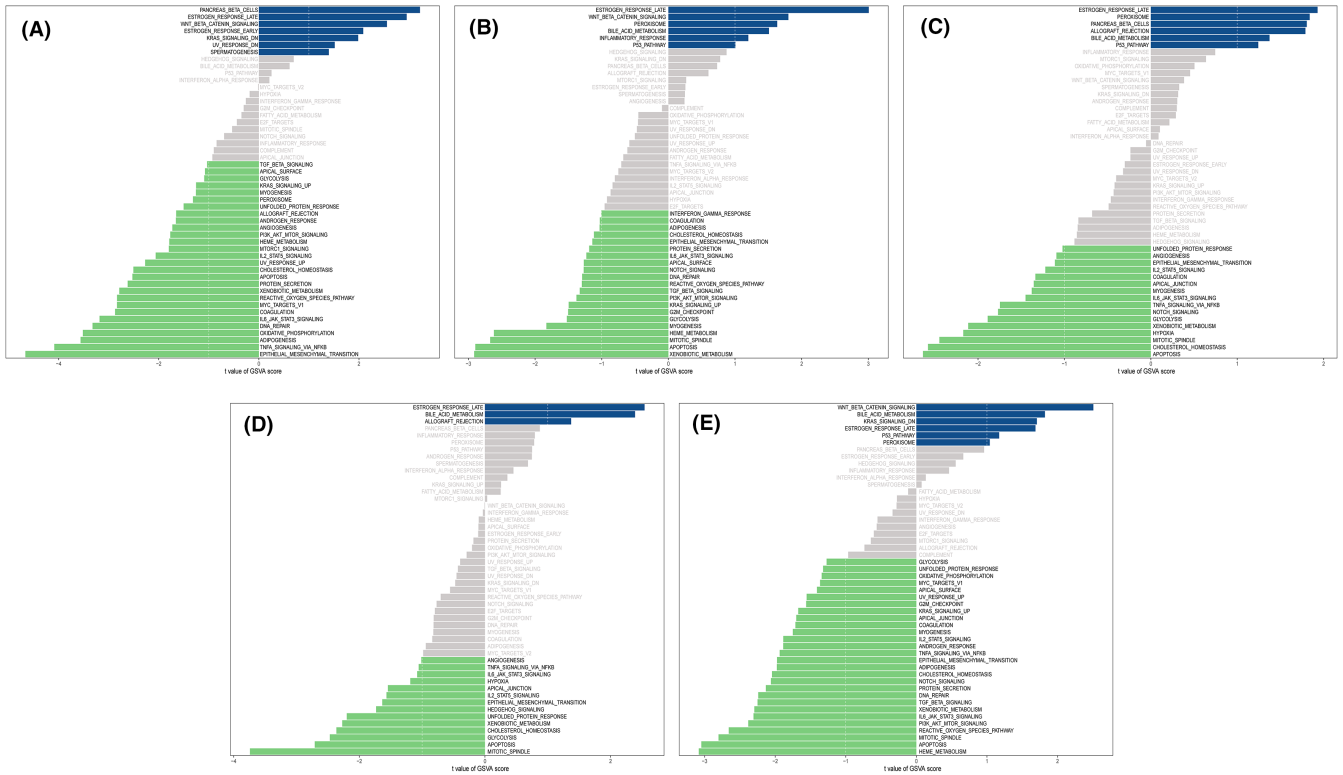
FIGURE 4 Gene set variation analysis analysis. (A) GAPDH-enriched pathways. (B) PF4-enriched pathways. (C) SELP-enriched pathways. (D) APP-enriched pathways. (E) PPBP-enriched pathways
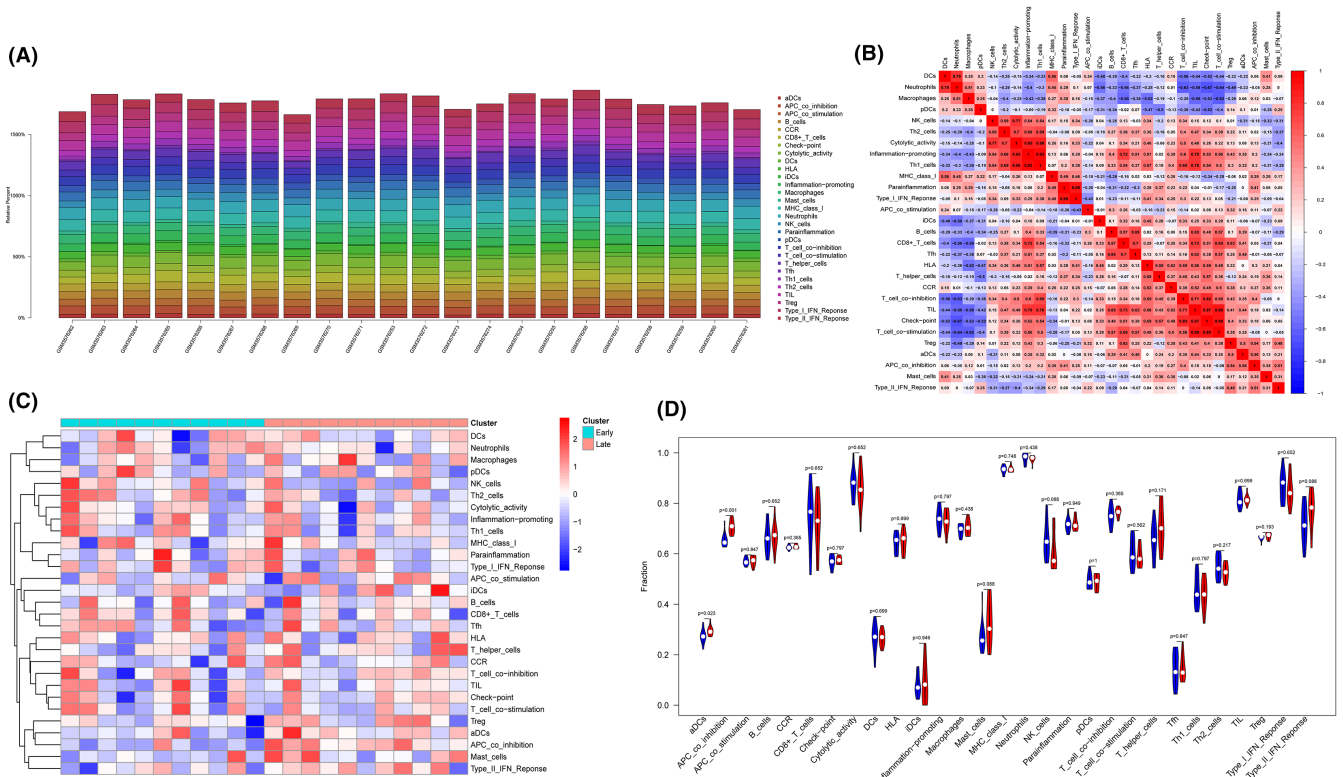
FIGURE 5 The landscape of immune infiltration in two subtypes of ICH samples. (A) The relative percentage of 29 subpopulations of immune signatures in 22 samples from GSE125512. (B) The heat map of the Correlation among 29 types of immune signatures. (C) Landscape evaluation of 29 types of immune signatures in two subgroups of ICH samples. (D) The Violin diagram showed the difference of immune infiltration between early and late groups according to dynamic changes of ICH. The early controls group was marked as blue, and the late group was marked as red (*p* < 0.05 was regarded as statistical significance)
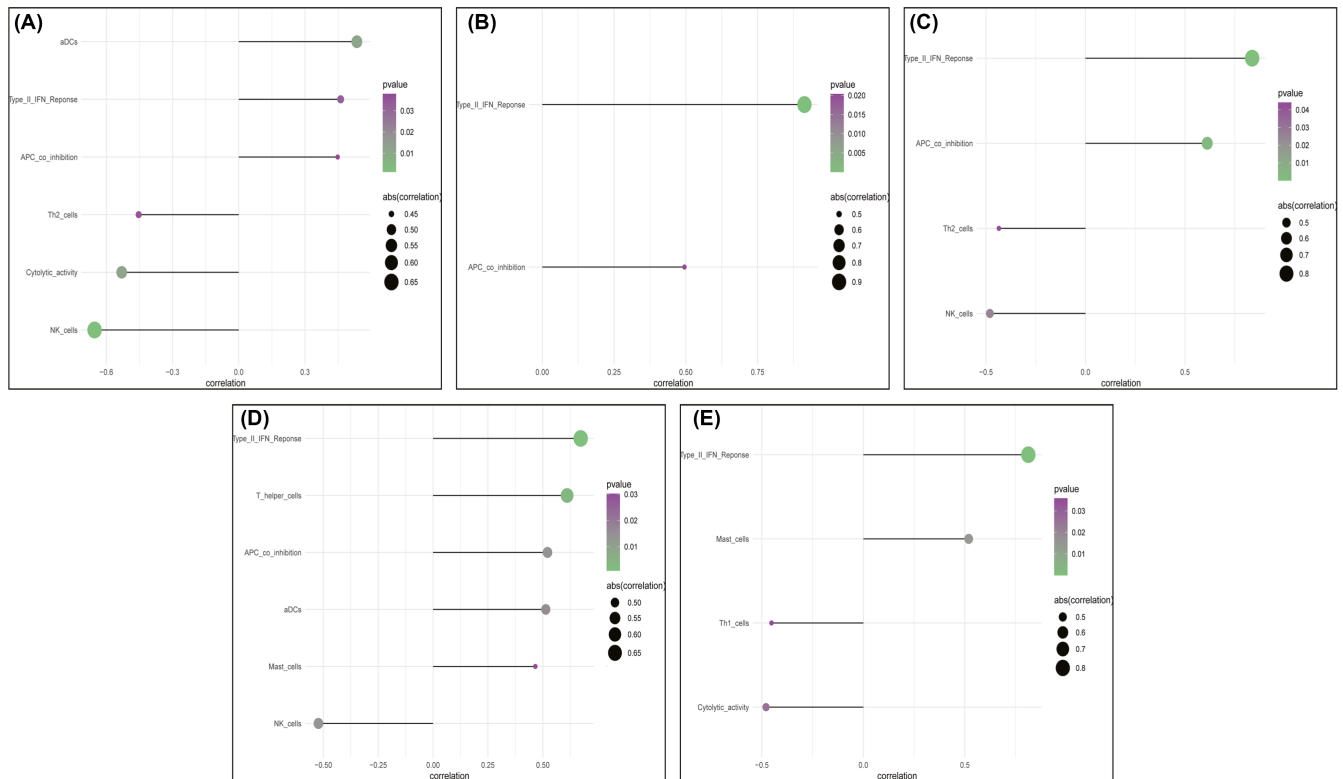
FIGURE 6 Correlation between five hub genes and immune signatures. (A) Correlation between GAPDH and infiltrating immune signatures. (B) Correlation between PF4 and infiltrating immune signatures. (C) Correlation between SELP and infiltrating immune signatures. (D) Correlation between APP and infiltrating immune signatures. (E) Correlation between PPBP and infiltrating immune signatures. The size of the dots represented the strength of the Correlation between genes and immune signatures; the more significant the dots, the stronger the Correlation. The color of the dots represented the *p*-value; the greener the color, the lower the *p*-value, and the purpler the color, the larger the *p*-value. *p* < 0.05 was considered statistically significant

types with an overall trend of up-regulation.[20] Besides, the role of GAPDH in immunity had also been explored. Hypoxia activates HIF-1α transcription factor and upregulates GAPDH expression. The upregulation of GAPDH may enhance the transcription and activity of HIF-1α, ultimately limiting the accumulation of immune cells such as CD8+ T lymphocytes.[21] In addition, the function of immune cells is affected by metabolic status. Both cytotoxic T cells and effector T cells dependent on glycolysis can be inhibited in low glucose and high lactate environments.[22] Therefore, the modulation of GAPDH activity has the potential to be a new approach for the treatment of immunosuppression. Over the years, researchers have moved from platelets' roles in maintaining homeostasis and thrombosis to their roles in inflammation and immunity.[23] Platelet-expressed receptors release a wide range of inflammatory mediators and have been shown to be involved in inflammation, immunity, and tissue repair.[24] Among the pathogenesis of many diseases, platelets show exciting prospects in the field of neuropathology, especially for stroke.[25,26] PF4 (Platelet factor 4), also known as CXCL4, has been detected in the serum of patients suffering from stroke.[27] It has been demonstrated to be expressed in microglia both in vitro and in vivo. In the stroke model, the researchers found that PF4 could attract microglia or other immune cells to the site of injury.[28] SELP (P-selectin) as one of cell adhesion molecules discovered, mainly mediates platelet activation, endothelial cell adhesion and interaction with white blood cells, and is closely related to immune injury, inflammation, thrombosis, and tumor metastasis.[29,30] Studies on cerebrovascular diseases had found that when cerebrovascular endothelium was damaged, the expression of SELP in platelets and endothelial cells increased, and then binds with P-selectin glycoprotein ligand-1 (PSGL-1) on leukocytes to activate signal transduction in leukocytes, causing leukocytes to release inflammatory factors and aggravate inflammatory responses.[31] Besides, PSGL-1 and E/P-selectins were essential for T-cell rolling in inflamed CNS microvessels.[32] APP (amyloid precursor protein) as the source of the amyloid β peptide, has been principally known and studied for its involvement in Alzheimer's disease. However, its main physiological function in the nervous system has not been fully studied.[33] Partial mutation of APP can lead to increased Aβ production, or Aβ more prone to aggregation. The accumulation of Aβ leads to the disorder of cellular calcium signaling and malfunctioning of mitochondria, which in turn leads to the loss of synapses and the death of neurons, as well as a series of neuroinflammation.[34] There was little research on the role of APP in ICH, especially the immune mechanism involved in the progression of cerebral hemorrhage. Therefore, APP as a potential target deserves further study. PPBP (pro-platelet basic protein) or chemokine (C-X-C motif) ligand 7 (CXCL7) is an encoded protein, which belongs to the

platelet growth factor of the CXC chemotherapy family. PPBP is released from activated platelets and is proved to be potential novel biomarker for multiple tumors.[35,36] It had been demonstrated that in breast cancer, PPBP, as an important immune cytokine, was secreted by tumor monocytes and played an important role in cancer cell migration, invasion, and metastasis. After PPBP antibody was administered, the abundance of M2 macrophages in the tumor microenvironment was significantly reduced, which reduced tumor growth and distant metastasis.[37] PPBP had also been shown to be involved in immune regulation and promotion of inflammatory progression in brain injury.[38] Given that the hub genes involved in handling immune cells and closely related to the infiltration level in the progress of ICH. Besides, functional enrichment analysis indicated inflammation was relevant to the pathophysiology of ICH. Thus, we believed that the immune response was likely to participate in ICH's pathological process and progress.

Neutrophils are the early peripheral blood cells to penetrate the perihematomal brain and the hematoma after ICH.[39] Neutrophils cause BBB damage, activation of resident microglia, and induce brain injury at early times following ICH.[40] T lymphocytes, a component of the adaptive immune system, regulate the immune response or evoke cytotoxicity. T lymphocytes have been identified in perihematomal brain tissue of ICH patients, and Treg transfer reduces neurological deficits in experimental ICH.[41] Moreover, the circulating CD4+/CD8+T lymphocyte ratio has been proposed as a possible predictor of postoperative intracranial pressure and short-term prognosis.[42] Regulatory T cells meliorate BBB breakdown after stroke.[43] This study first mapped the infiltration levels of neutrophils and CD8+ T lymphocytes in all patients with ICH based on the ssGSEA method.

In the present study, five hub genes were identified, and their dynamic expression changes were validated, accompanied by the progress of ICH. The identified genes' biological functions and pathways provided a better-detailed understanding of inflammation and immunity for ICH development. By coupling WGCNA, metascape, GSVA algorithm, and ssGSEA method, we speculated that these five hub genes might affect the development of ICH through the immune mechanism. These conclusions may help improve immunomodulatory therapies for ICH patients. However, our research was the second mining and analysis of previously published data. The reliability of the present study needs to be validated by further in vivo and in vitro experiments.

5 | CONCLUSIONS

We identified the royal blue module as the most relevant module to the disease progression of ICH and finally screened five hub genes (GAPDH, PF4, SELP, APP, and PPBP) in the royal blue module. Metascape analysis displayed the biological processes related to inflammation and immunology. These findings may help us better understand the pathophysiological mechanisms of ICH by exploring the dynamic changes of hub genes. From the immune system's perspective, evaluating the infiltration of immune cells and determining the differences in the composition of infiltrating immune cells would be of great value for us to improve immunomodulatory therapies for ICH patients.

CONFLICT OF INTEREST

The authors declare no conflict of interest.

AUTHOR CONTRIBUTIONS

Hao Guo and Hongyin Du: Conceptualization, methodology, and software; Hao Guo, Yanjun Zhang and Zhanfei Hu: Data curation, writing original draft; Yanjun Zhang: Visualization, investigation; Li Wang: Supervision; Zhanfei Hu: Software and validation; Hongyin Du: Writing, reviewing, and editing.

DATA AVAILABILITY STATEMENT

The data sets analyzed in this manuscript are publicly available. The data set is available on the Gene Expression Omnibus (GEO) database, and the accession number is GSE125512.

ORCID

Hongyin Du https://orcid.org/0000-0002-9505-8947

REFERENCES

1. Keep RF, Hua Y, Xi G. Intracerebral haemorrhage: mechanisms of injury and therapeutic targets. *Lancet Neurol.* 2012;11(8):720-731.
2. An SJ, Kim TJ, Yoon BW. Epidemiology, risk factors, and clinical features of intracerebral hemorrhage: an update. *J Stroke.* 2017;19(1):3-10.
3. Sacco S, Marini C, Toni D, Olivieri L, Carolei A. Incidence and 10-year survival of intracerebral hemorrhage in a population-based registry. *Stroke.* 2009;40(2):394-399.
4. Rincon F, Mayer SA. Clinical review: critical care management of spontaneous intracerebral hemorrhage. *Crit Care.* 2008;12(6):237.
5. Zhou Y, Wang Y, Wang J, Anne Stetler R, Yang QW. Inflammation in intracerebral hemorrhage: from mechanisms to clinical translation. *Prog Neurogibol.* 2014;115:25-44.
6. Xi G, Keep RF, Hoff JT. Mechanisms of brain injury after intracerebral haemorrhage. *Lancet Neurol.* 2006;5(1):53-63.
7. Aronowski J, Zhao X. Molecular pathophysiology of cerebral hemorrhage: secondary brain injury. *Stroke.* 2011;42(6):1781-1786.
8. Li YJ, Chang GQ, Liu Y, et al. Fingolimod alters inflammatory mediators and vascular permeability in intracerebral hemorrhage. *Neurosci Bull.* 2015;31(6):755-762.
9. Lee ST, Chu K, Jung KH, et al. Memantine reduces hematoma expansion in experimental intracerebral hemorrhage, resulting in functional improvement. *J Cereb Blood Flow Metab.* 2006;26(4):536-544.
10. Zhou K, Zhong Q, Wang YC, et al. Regulatory T cells ameliorate intracerebral hemorrhage-induced inflammatory injury by modulating microglia/macrophage polarization through the IL-10/GSK3beta/PTEN axis. *J Cereb Blood Flow Metab.* 2017;37(3):967-979.

11. Langfelder P, Horvath S. WGCNA: an R package for weighted correlation network analysis. *BMC Bioinformatics*. 2008;9:559.

12. Zhang B, Horvath S. A general framework for weighted gene co-expression network analysis. *Stat Appl Genet Mol Biol*. 2005;4(1):1-45.

13. Zhou Z, Cheng Y, Jiang Y, et al. Ten hub genes associated with progression and prognosis of pancreatic carcinoma identified by co-expression analysis. *Int J Biol Sci*. 2018;14(2):124-136.

14. Zhou Y, Zhou B, Pache L, et al. Metascape provides a biologist-oriented resource for the analysis of systems-level datasets. *Nat Commun*. 2019;10(1):1523.

15. Subramanian A, Tamayo P, Mootha VK, et al. Gene set enrichment analysis: a knowledge-based approach for interpreting genome-wide expression profiles. *Proc Natl Acad Sci USA*. 2005;102(43):15545-15550.

16. Hanzelmann S, Castelo R, Guinney J. GSVA: gene set variation analysis for microarray and RNA-seq data. *BMC Bioinformatics*. 2013;14:7.

17. Li W, Li L, Li W, et al. Spleen associated immune-response mediates brain-heart interaction after intracerebral hemorrhage. *Exp Neurol*. 2020;327:113209.

18. Shi K, Tian DC, Li ZG, Ducruet AF, Lawton MT, Shi FD. Global brain inflammation in stroke. *Lancet Neurol*. 2019;18(11):1058-1066.

19. Sirover MA. New insights into an old protein: the functional diversity of mammalian glyceraldehyde-3-phosphate dehydrogenase. *Biochim Biophys Acta*. 1999;1432(2):159-184.

20. Guo C, Liu S, Sun MZ. Novel insight into the role of GAPDH playing in tumor. *Clin Transl Oncol*. 2013;15(3):167-172.

21. Chiche J, Pommier S, Beneteau M, et al. GAPDH enhances the aggressiveness and the vascularization of non-Hodgkin's B lymphomas via NF-Kb-dependent induction of HIF-1α. *Leukemia*. 2015;29:1163-1176.

22. Quinn WJ 3rd, Jiao J, TeSlaa T, et al. Lactate limits T cell proliferation via the NAD(H) Redox State. *Cell Rep*. 2020;33(11):108500.

23. Sonia D'Souza C, Li Z, Luke Maxwell D, et al. Platelets drive inflammation and target gray matter and the retina in autoimmune-mediated encephalomyelitis. *J Neuropathol Exp Neurol*. 2018;77(7):567-576.

24. Nording HM, Seizer P, Langer HF. Platelets in inflammation and atherogenesis. *Front Immunol*. 2015;6:98.

25. Nieswandt B, Kleinschnitz C, Stoll G. Ischaemic stroke: a thromboinflammatory disease? *J Physiol (Lond)*. 2011;589:4115-4123.

26. Stoll G, Kleinschnitz C, Nieswandt B. Molecular mechanisms of thrombus formation in ischemic stroke: novel insights and targets for treatment. *Blood*. 2008;112:3555-3562.

27. Shah AB, Beamer N, Coull BM. Enhanced in vivo platelet activation in subtypes of ischemic stroke. *Stroke*. 1985;16(4):643-647.

28. de Jong EK, de Haas AH, Brouwer N, et al. Expression of CXCL4 in microglia in vitro and in vivo and its possible signaling through CXCR3. *J Neurochem*. 2008;105(5):1726-1736.

29. Zheng C, Ricci J, Zhang Q, et al. Characterization of novel p-selectin targeted complement inhibitors in murine models of hindlimb injury and transplantation. *Front Immunol*. 2021;12:785229.

30. Mocanu CA, Fuior EV, Voicu G, et al. P-selectin targeted RAGE-shRNA lipoplexes alleviate atherosclerosis-associated inflammation. *J Control Release*. 2021;338:754-772.

31. Tinoco R, Otero DC, Takahashi AA, Bradley LM. PSGL-1: a new player in the immune checkpoint landscape. *Trends Immunol*. 2017;38(5):323-335.

32. Sathiyanadan K, Coisne C, Enzmann G, Deutsch U, Engelhardt B. PSGL-1 and E/P-selectins are essential for T-cell rolling in inflamed CNS microvessels but dispensable for initiation of EAE. *Eur J Immunol*. 2014;44(8):2287-2294.

33. Cho Y, Bae HG, Okun E, Arumugam TV, Jo DG. Physiology and pharmacology of amyloid precursor protein. *Pharmacol Ther*. 2022;235:108122.

34. Luu L, Ciccotosto GD, Cappai R. The Alzheimer's disease amyloid precursor protein and its neuritogenic actions. *Curr Alzheimer Res*. 2021;18(10):772-786.

35. Li L, Zhang L, Zhang T, Qi X, Cheng G, Xia L. Serum chemokine CXCL7 as a potential novel biomarker for obstructive colorectal cancer. *Front Oncol*. 2021;10:599363.

36. Kinouchi T, Uemura M, Wang C, et al. Expression level of CXCL7 in peripheral blood cells is a potential biomarker for the diagnosis of renal cell carcinoma. *Cancer Sci*. 2017;108(12):2495-2502.

37. Wang YH, Shen CY, Lin SC, et al. Monocytes secrete CXCL7 to promote breast cancer progression. *Cell Death Dis*. 2021;12(12):1090.

38. Lu S, Kong W, Wang S. Exploring the changes of brain immune microenvironment in Alzheimer's disease based on PANDA algorithm combined with blood brain barrier injury-related genes. *Biochem Biophys Res Commun*. 2021;557:159-165.

39. Zhao X, Sun G, Zhang H, et al. Polymorphonuclear neutrophil in brain parenchyma after experimental intracerebral hemorrhage. *Transl Stroke Res*. 2014;5(5):554-561.

40. Sun N, Shen Y, Han W, et al. Selective sphingosine-1-phosphate receptor 1 modulation attenuates experimental intracerebral hemorrhage. *Stroke*. 2016;47(7):1899-1906.

41. Mracsko E, Veltkamp R. Neuroinflammation after intracerebral hemorrhage. *Front Cell Neurosci*. 2014;8:388.

42. Su W, Gao C, Wang P, et al. Correlation of circulating T lymphocytes and intracranial hypertension in intracerebral hemorrhage. *World Neurosurg*. 2017;107:389-395.

43. Li P, Gan Y, Sun BL, et al. Adoptive regulatory T-cell therapy protects against cerebral ischemia. *Ann Neurol*. 2013;74(3):458-471.